THE JOURNAL OF PHYSICAL CHEMISTRY C

Article

pubs.acs.org/JPCC

Luminescent Metal-Nucleobase Network Thin Films by Atomic/Molecular Layer Deposition

Zivile Giedraityte,[†] Jani Sainio,[‡] Dirk Hagen,[†] and Maarit Karppinen*,[†]

[†]Department of Chemistry and Materials Science, and [‡]Department of Applied Physics, Aalto University, FI-00076 Aalto, Finland

ABSTRACT: Controlled molecular deposition of natural organic molecules such as nucleobases (NBs) into well-defined thin films represents progress toward exciting new nanomaterials. The strongly emerging atomic/molecular layer deposition (ALD/MLD) technique provides us with an elegant way to realize the depositions through gas phase with atomic/molecular level accuracy. In the resultant thin films the organic molecules are bound together not only with hydrogen bonds but also via metal cation linkers and are likely to exhibit novel properties. Here we demonstrate the ALD/MLD of such thin films with monovalent sodium, divalent barium, or trivalent lanthanum as the metal linker and uracil or adenine as the NB component. Our metal-NB thin films are homogeneous, smooth, and in the case of sodium and barium also crystalline showing intense photoluminescence. We discuss the impact of the size and charge of the metal cation on the growth and properties of the films.

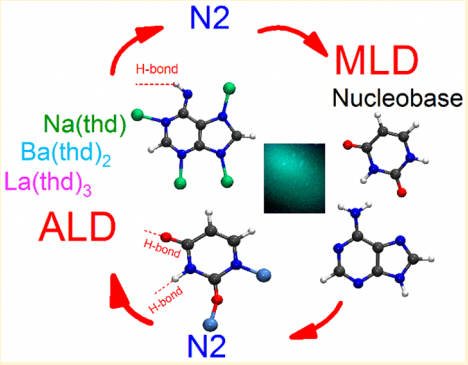

1. INTRODUCTION

Combining biobased organic components with inorganics into advanced functional materials with unorthodox (synergistic or collective) physical properties could be transformational for the next-generation applications in, e.g., electronics, optics, or sensing. However, new approaches are required to realize the dream of rationally constructing such materials from different building blocks into desired functionality.[1]

Deoxyribonucleic acid (DNA) and ribonucleic acid (RNA) are widely studied as exciting sustainable biobased precursors for the hybrid bio-organic−inorganic materials.[2,3] Equally exciting precursors could be the simple molecular constituents of DNA and RNA, that is, the five different nucleobase (NB) molecules.[4] They have several attractive features, including their tendency to organize into larger supramolecular assemblies via hydrogen bonds.[5−9] There are also interesting studies reported involving the interactions of NBs with different metal ions and resulting in the formation of various assemblies depending on the participating metal atom/molecule pairs.[10−12] It is interesting to recall that metal−nucleic acid interactions are involved in genetic information storage and transfer; also interestingly, through nanostructuring researchers have created, e.g., nucleic acids sensors.[13] It should be emphasized that the different NBs would form an abundant raw material source for our next-generation devices as they can be obtained both naturally and synthetically.

The relatively small size of the NB molecules is a clear advantage considering the possible routes to combine the bio-organic component with the inorganic component for the hybrid material, as it allows the sublimation of NBs to gas phase and thereby the use of the most advanced gas-phase thin-film deposition techniques originally developed for inorganic materials. Indeed, we recently demonstrated the fabrication of crystalline sodium-uracil thin films[14] using the strongly emerging combined atomic and molecular layer deposition (ALD/MLD) technique.[15−19] On the other hand, in our recent works, we have also developed novel ALD/MLD processes for other types of crystalline hybrid thin films based on alkali (Li) and alkaline earth (Ca) metals having an eye on potential Li-ion microbattery[20] and metal organic framework[21,22] applications, but the work on the Na-uracil thin films was the first ALD/MLD work involving NBs. In the present work we aim to extend the approach from monovalent alkali metal species to divalent alkaline earth (Ba) and trivalent lanthanide (La) species as the metal constituent in metal-NB thin films; our anticipation is that not only the cation valence but also the larger size of Ba and La in comparison to Na might affect the metal-nucleobase coordination and thereby possibly also the properties of the films. For the NB constituent we investigate not only uracil but also adenine that, unlike uracil, does not have hydroxide groups, see Figure 1. Besides the new ALD/MLD processes, we report photoluminescence properties for our metal-NB thin films.

2. EXPERIMENTAL SECTION

The hybrid Na-, Ba-, and La-nucleobase thin films were grown in a commercial ALD reactor (F-120 by ASM Microchemistry Ltd.). As precursors, in-house synthesized Na(thd), $Ba(thd)_2$, and $La(thd)_3$ (thd: 2,2,6,6-tetramethyl-3,5-heptadionate) and commercial uracil and adenine (Sigma-Aldrich) were used; these solid precursors were sublimated from open precursor boats at the following temperatures: Na(thd) 195 °C, $Ba(thd)_2$ 205 °C, $La(thd)_3$ 167 °C, uracil 235 °C, and adenine 255 °C.

Received: June 22, 2017
Revised: July 26, 2017
Published: July 26, 2017

DOI: 10.1021/acs.jpcc.7b06129
J. Phys. Chem. C 2017, 121, 17538−17545

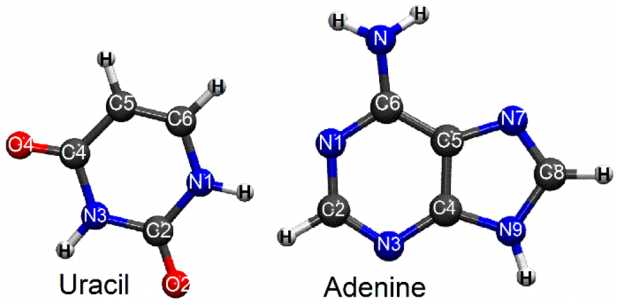

Figure 1. Structures of the nucleobase precursor molecules employed: uracil $C_4H_4N_2O_2$ and adenine $C_5H_5N_5$.

Nitrogen (99.999%; Schmidilin UHPN 3000 N_2 generator) was used as a carrier gas for the precursors and also for purging the reactor chamber after each precursor pulse, and its pressure was kept at 2−4 mbar during the film deposition. As the first step of process optimization, the precursor and purge pulse lengths were investigated for the $Ba(thd)_2$ + uracil process within 1.5−3.5 s $Ba(thd)_2$/2−7 s N_2/2−4 s uracil/4−8 s N_2. Based on these depositions and some preliminary experiments with the other precursor pairs the pulse and purge periods were fixed at the following values for all other depositions: 1.5 s metal precursor/2 s N_2/2 s NB/4 s N_2. The first depositions were carried out at different temperatures from 260 to 320 °C, but for the final depositions the temperature was fixed to 300 °C for the better comparison. Both silicon and quartz substrates were used.

For the film thickness and density evaluation, we used X-ray reflectivity measurements (XRR; Analytical Pert MPD Pro Alfa; Cu $K\alpha_1$ radiation). Grazing incidence X-ray diffraction (GIXRD) measurements were performed with the same equipment to address the crystallinity of the films. Surface morphology was investigated with atomic force microscopy (AFM; Veeco Dimension 51000 Scanning Probe Microscope; Nanoscope Controller, Digital Instruments, Inc.; Nanoscope Analysis 1.5 Software). Moreover, for the Na-based films which turned out to be rougher than the other films, the cantilever AFM tip jump was used to estimate the film thickness (instead of the XRR data).[14]

Chemical composition and bonding characteristics of the films were investigated by Fourier transform infrared spectroscopy (FTIR; Nicolet 380, ThermoFisher Scientific) and X-ray photoelectron spectroscopy (XPS; Kratos Axis Ultra spectrometer). In both cases our uracil precursor powder was used as a reference sample. The FTIR spectra we recorded in transmission mode with a 1 cm^{-1} resolution and averaged over a minimum of 64 scans. The XPS spectra were acquired with monochromated Al $K\alpha$ radiation and charge neutralization. High resolution spectra were measured using a pass energy of 20 eV, an X-ray power of 75 W, and an analysis area of approximately 700 × 300 μm^2. The nitrogen 1s peak of uracil at 400.9 eV was used as a reference to correct for charging the samples. Due to surface oxidation, for Ba-adenine the spectra were collected after sputtering away ca. 3 nm of the film with an Ar gas cluster ion source (Kratos Analytical; Ar_{500}^+ clusters; 10 keV).

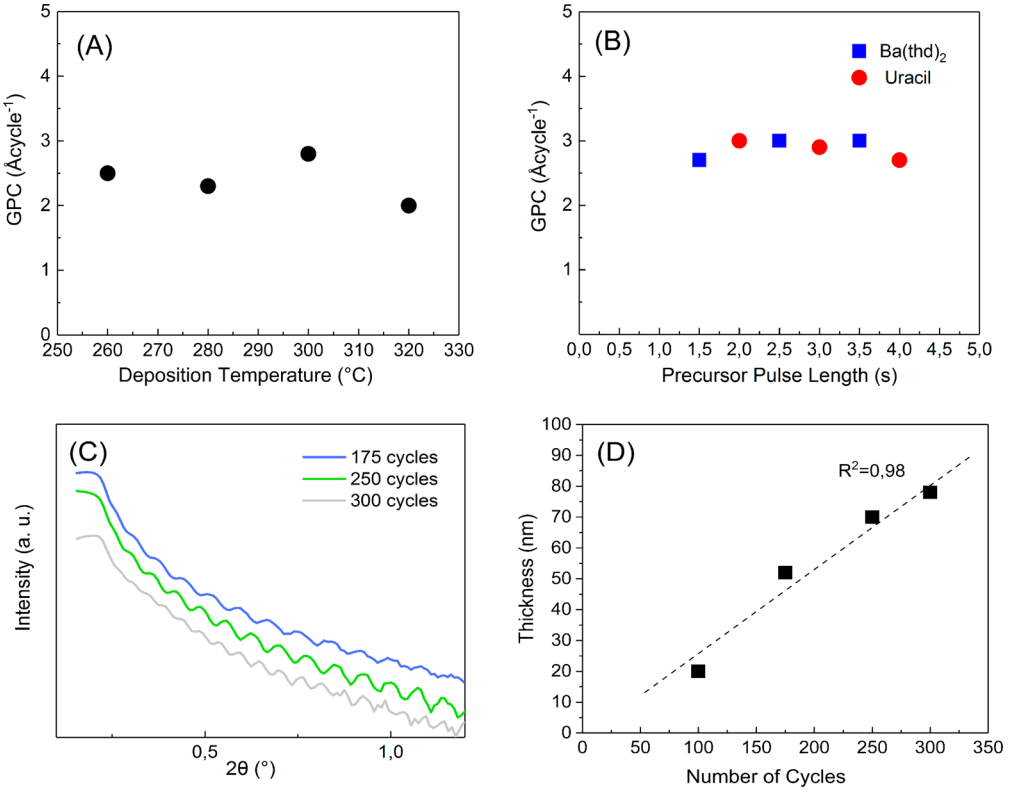

Figure 2. Optimization of the deposition parameters and confirmation of the ALD/MLD type film growth for our $Ba(thd)_2$ + uracil process (estimated error bars within the datum point marks): (A) GPC at different deposition temperatures; (B) GPC with different precursor pulse lengths; (C) examples of XRR curves for films deposited with different numbers of ALD/MLD cycles; (D) linear dependence of the film thickness on the number of ALD/MLD cycles. In panels B−D the deposition temperature was 300 °C.

DOI: 10.1021/acs.jpcc.7b06129
J. Phys. Chem. C 2017, 121, 17538−17545

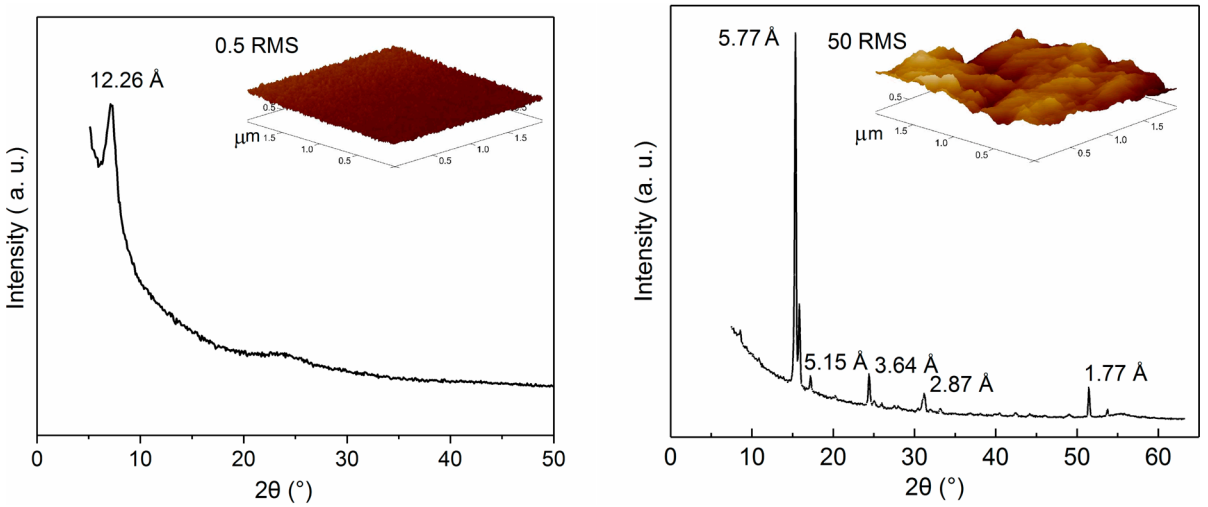

Figure 3. GIXRD patterns and AFM images for the Ba-uracil (thickness 70 nm) and Na-adenine (thickness 200 nm) films.

For the characterization of our metal-nucleobase thin films for their photoluminescence properties both excitation and emission spectra were collected by Quanta Master 40 spectrofluorometer from Photon Technology International; in these measurements the second order peaks were eliminated by using a 400−495 nm long pass filter (FGL400, FGL495, Thorlabs) in the emission channel. The emission and excitation slits were set to 1.25 nm, and the fluorescence spectra were corrected by using instrument's excitation and emission corrections provided by the manufacturer. Finally, UV−vis absorption spectra were measured for the samples using PerkinElmer Lambda 950 UV/vis/NIR absorption spectrophotometer.

Finally we deposited Ba-uracil on porous substrates of anodized aluminum oxide (AAO; InRedox; 1 μm deep, 300 nm pore diameter). These depositions were carried out at 300 °C for 250 ALD/MLD cycles of the pulse sequence, 1.5 s $Ba(thd)_2$/2 s N_2/2 s uracil/4 s N_2, to target the film thickness of 70.8 nm. Scanning electron microscopy (SEM; Zeiss Sigma VP microscope; seconday electron detector at 2.5 kV; Carl Zeiss Microscopy Ltd.) images were taken to investigate the conformity of the coatings.

3. RESULTS AND DISCUSSION

Among the different metal precursor and NB precursor pairs tested, we optimized the ALD/MLD thin-film growth parameters most thoroughly for the $Ba(thd)_2$ + uracil process, as summarized in Figure 2. An almost constant growth-per-cycle (GPC) value of ∼2.8 Å/cycle was observed within the entire deposition temperature range studied, i.e., 260−320 °C, and also essentially independent of the lengths of the precursor pulses. For the rest of experiments we fixed the deposition temperature at 300 °C and used the following pulse/purge lengths in our ALD/MLD cycle: 1.5 s $Ba(thd)_2$/2 s N_2/2 s uracil/4 s N_2. This process yielded a linear dependence for the film thickness on the number of ALD/MLD cycles, demonstrating that the thickness indeed can be controlled by the number of ALD/MLD cycles. With these characteristics we can conclude that our $Ba(thd)_2$ + uracil process fulfils the basic criteria considered for an ideal ALD/MLD process. Moreover, based on a less systematic mapping of the deposition parameters for the other precursor combinations, we could conclude that the aforementioned parameters yielded homogeneous films in a reproducible manner for all of the other precursor pairs as well.

All our ALD/MLD processes yielded relatively smooth metal-NB thin films; only the highly crystalline Na-adenine films were less smooth. We estimated the surface roughness values for the Ba-uracil films from both XRR (Figure 2) and AFM (Figure 3) data in a rather good mutual agreement: both techniques gave values close to 0.5 nm for the surface roughness of ca. 70 nm thick films.

Crystallinity of the films was found to depend on the choice of the metal constituent in such a way that both the La-NB films were clearly amorphous, the Ba-NB films were at least partly crystalline, and the Na-NB films well crystalline. In Figure 3 we display the GIXRD patterns for two representative samples, i.e., a 70 nm thick Ba-uracil film and a 200 nm thick Na-adenine film. In the latter Na-adenine case, there are several sharp diffraction peaks while in the former Ba-uracil case only one clear low-angle peak is seen besides some broad features at the higher angles. In both the cases, the observed peaks/patterns cannot be explained by any known Na−C−H−N−O or Ba−C−H−N−O structure which is rather natural as we believe that the ALD/MLD technique has the capacity to produce fundamentally new types of metal-nucleobase hybrid materials. We may thus only compare the low-angle d values observed for the different metal-NB films, see Table I. Just tentatively, taking the larger size of Ba in comparison to Na, and adenine in comparison to uracil into account, the d values for the different crystalline hybrid materials look reasonable.

Table I. Growth-per-Cycle Values and GIXRD Peak Positions for the Metal-NB Thin Films Investigated

metal	NB	GPC [Å/cycle]	d [Å] of GIXRD peak
Na	uracil	4.8 (AFM)	11.5
Ba	uracil	2.8	12.2
La	uracil	1.6	amorphous
Na	adenine	∼10 (AFM)	5.8
Ba	adenine	3.4	(nearly) amorphous
La	adenine	1.4	amorphous

Before discussing the properties of our metal-NB thin films further, it is interesting to compare the GPC values for the different processes (Table I). The GPC values for the two

DOI: 10.1021/acs.jpcc.7b06129
J. Phys. Chem. C 2017, 121, 17538−17545

$La(thd)_3$ + NB processes (1.6 and 1.4 Å/cycle for uracil and adenine, respectively) are significantly lower than the values for the two $Ba(thd)_2$ + NB processes (3.0 and 3.4 Å/cycle) which in turn are lower than the values for the two Na(thd) + NB processes (4.8 and ~10 Å/cycle). This trend strongly suggests that the growth rate is apparently controlled by steric hindrance of the bulky thd ligands of the metal precursors, such that the GPC value decreases when the number of these ligands increases in the order of Na(thd), $Ba(thd)_2$, and $La(thd)_3$.

For the chemical composition of the films, a rough estimation can be obtained from the XPS survey spectra collected for the Ba-uracil and Ba-adenine films, see Figure 4.

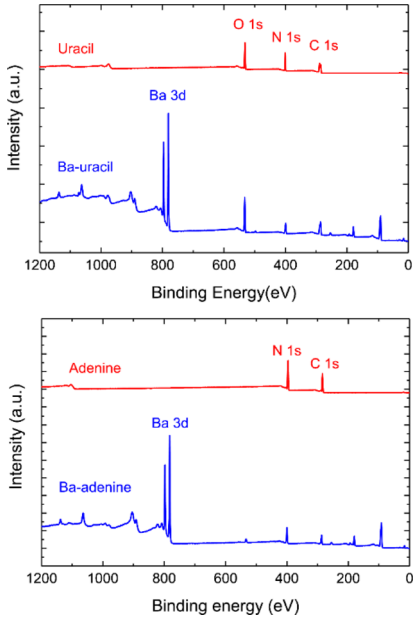

Figure 4. XPS survey spectra for the Ba-uracil and Ba-adenine thin films as well as for the uracil and adenine precursors for comparison.

First of all, no other elements than expected were found in the samples. The concentrations (calculated from peak areas of high resolution spectra; in at-%) for uracil $C_4H_4N_2O_2$ (55 C, 24 N, 21 O) and Ba-uracil (53 C, 15 N, 25 O, 7 Ba) are nearly stoichiometric and would suggest bonding of one barium atom per uracil molecule in our Ba-uracil film. The somewhat decreased proportion of nitrogen found for Ba-uracil could be at least partly due to carbon and oxygen contamination on the thin-film surface. For adenine $C_5H_5N_5$ (52 C, 48 N, 0.2 O) and Ba-adenine (40 C, 36 N, 18 Ba, 6 O) similar carbon and oxygen excess/contamination is seen as well. Nevertheless, we may estimate the Ba:adenine ratio at around two in our Ba-adenine thin film. The density for the Ba-uracil and Ba-adenine films was determined to be 2.6 and 2.0 g/cm^3, respectively, from XRR measurements.

To get insights into the types of chemical bonding in different metal-NB materials, we carried out FTIR measurements for all our hybrid thin films and also for the uracil and adenine precursors for comparison. The spectra are shown in Figure 5. We first discuss the metal-uracil films. Overall, it can be seen that the spectra for all three metal-uracil films show many common features: the Ba- and La-uracil spectra are nearly identical, whereas the Na-uracil spectrum is somewhat different. From literature related to uracil-based metal complexes it is known that C2═O and C4═O are the most preferable binding sites for uracil.[23] This seems to be the case also in our metal-uracil thin films. Namely, the bands due to ν(C2═O) and ν(C4═O+C═C) seen for pure uracil at 1710 and 1675 cm^{-1}, respectively, essentially disappear for Ba- and La-uracil indicating that both C2═O and C4═O are strongly involved in bonding. Also for Na-uracil these bands get weaker in intensity; moreover, the 1710 cm^{-1} band due to ν(C2═O) is shifted to 1699 cm^{-1}.

In the 1800−1300 cm^{-1} region featuring the N1−H and N3−H stretchings for the pure uracil, it is seen that changes take place for all three thin films as these peaks are shifted in each case. Finally, the O−H and N−H stretches seen in the 2800−3100 cm^{-1} region for uracil completely disappear for Ba- and La-uracil and get essentially weaker for Na-uracil; for the latter film also seen is broadening of the band around 3000 cm^{-1} apparently due to hydrogen bonding.[24] Hence we may conclude that in all three metal-uracil thin films all four functional sites of uracil, i.e., C2═O, C4═O, N1−H, and N3−H, are involved in bonding; whether these bonds are metal bonds or hydrogen bonds in each case remains somewhat ambiguous, though.

Then we discuss the FTIR data of our adenine-based samples. First of all, it seems that like in the case of uracil, also for the adenine series the Ba- and La-adenine spectra are more similar and the Na-adenine spectrum somewhat different. Nevertheless, for all three metal-adenine films the peak due to $-NH_2$ at 1670 cm^{-1} for pure adenine[25] moves upon the nucleobase-metal bond formation, to 1644 cm^{-1} for Na-adenine and to 1634 cm^{-1} for Ba- and La-adenine, confirming that the amino group is involved in bonding in all these films. Then, the signal at 1503 cm^{-1} assigned to N7 is shifted to 1542 cm^{-1} in the case of Na-adenine and to 1539 cm^{-1} for Ba- and La-adenine films, which shows that in all three materials the metal cation may bond to N7. In addition, the band at 1417.5 cm^{-1} (C4N9) shifts to 1379 cm^{-1} in the case of Na-adenine and to 1378 cm^{-1} for Ba- and La-adenine thin films which shows that all three metal-adenine films may bind through N9 as well. On the other hand, only for Na-adenine an additional peak is observed at 1475 cm^{-1} related to binding through N1.

To get additional insights into the bonding, we carried out high-resolution XPS measurements for our Ba-uracil sample at the N 1s, C 1s, and O 1s and Ba 1s regions; the spectra are shown in Figure 6 together with the corresponding spectra for the uracil precursor for comparison. In the latter case the features seen perfectly agree with previous literature.[26] Namely, the two inequivalent nitrogen atoms N1 and N3 of uracil are observed as one peak at 400.9 ± 0.1 eV in the N 1s spectrum, and the two oxygen atoms as one peak at 532.0 ± 0.1 eV in the O 1s spectrum.[27] The different carbon atoms on the other hand are resolved in the C 1s spectrum. For Ba-uracil, the Ba $3d_{5/2}$ peak observed at 780.7 ± 0.1 eV is consistent with various barium bonding environments, independent of the oxidation state of barium, it being Ba(II) or Ba(0).[26] The oxygen 1s peak is found at 532.0 ± 0.1 eV, i.e., essentially at the same energy as in the uracil reference. The most informative observation is that a new additional nitrogen peak appears at 399.1 ± 0.1 eV. We assign this feature to deprotonated N atom in the uracil molecule.[27,28] Such a deprotonation should cause changes in the C 1s spectrum as well. If, e.g., N3 is deprotonated, shifts of around−1 eV for the binding energies of C2 and C4 are to be expected.[27,28] From Figure 6, for our Ba-uracil the components C6 and C2 in particular have been shifted down in binding energy suggesting the deprotonation of N1. Also, simulta-

DOI: 10.1021/acs.jpcc.7b06129
J. Phys. Chem. C 2017, 121, 17538−17545

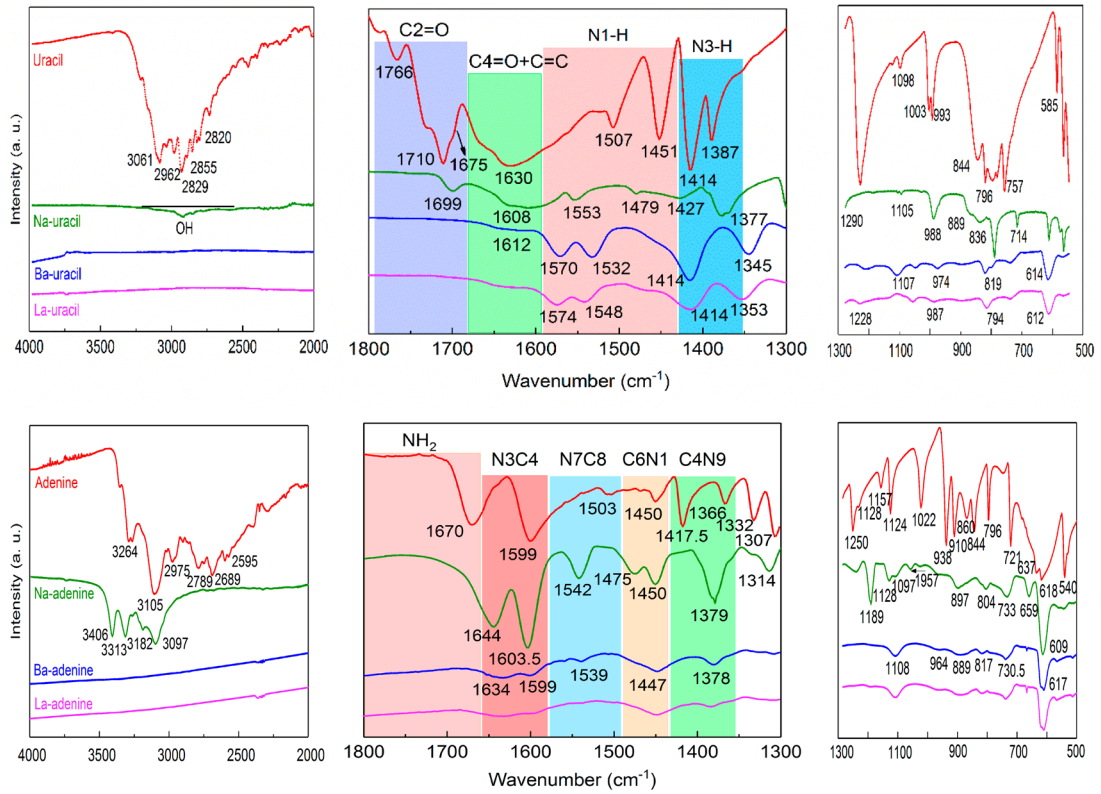

Figure 5. FTIR spectra for our metal-uracil (top) and metal-adenine (bottom) films and the corresponding NB precursors for comparison.

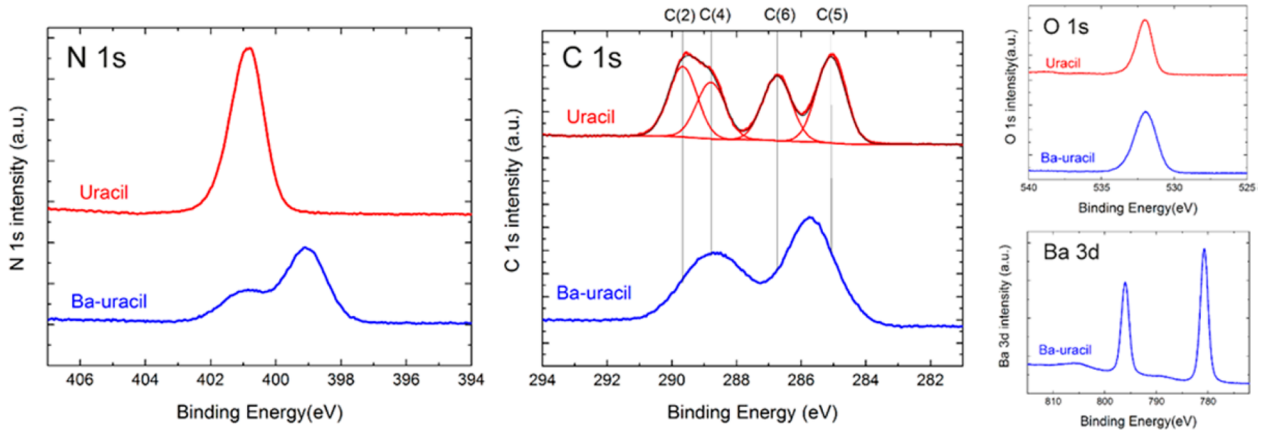

Figure 6. XPS spectra of the N 1s, C 1s, O 1s, and Ba 3d regions for uracil (top, red) and of Ba-uracil film (bottom, blue).

neously C5 seems to have been shifted to higher binding energies, suggesting that also other atoms could be involved in bonding. Earlier we revealed for our Na-uracil films similar although somewhat smaller shifts but suggesting toward the deprotonation of N3.[28] Hence, it is clear that in our metal-uracil thin films the metal ion is bonded not only to the C═O site(s) but also to the N atom(s). It should also be noted that in the N 1s spectrum more than half of the nitrogen found in the sample appears to be deprotonated. The XPS signal is however strongly surface sensitive so this ratio will also depend on the orientation of the uracil molecule with respect to the surface. To conclude our findings from the FTIR and XPS data for the bonding schemes in the different metal-NB thin films, it seems that different combinations of metal−oxygen, metal−nitrogen, and hydrogen bonds are involved. Additionally, we like to mention here that all of the metal-NB thin films investigated were found to be extremely stable even after long storage periods in open air. In particular, the La-uracil films could even be immersed in water; this extreme stability of La-uracil films is in line with another interesting observation for the same films, i.e., hydrophobicity with contact angle around 130°.

To discuss the optical properties of our metal-NB thin films we first show in the two upper panels of Figure 7 the UV absorption spectra for the metal-uracil and metal-adenine thin films, and also for the NB precursors for comparison. The well-known $\pi-\pi$ transition is seen at 262 and 260 nm for uracil and adenine, respectively. For all of the metal-NB thin films the absorption peak has been shifted toward the higher wavelengths, to 275/272 nm for Na-uracil/adenine and to 277/275 nm for both Ba- and La-uracil/adenine. Furthermore, for the metal-adenine films an additional absorption peak is seen at 320 nm for Na-adenine, at 378 nm for Ba-adenine and at 371 nm

DOI: 10.1021/acs.jpcc.7b06129
J. Phys. Chem. C 2017, 121, 17538−17545

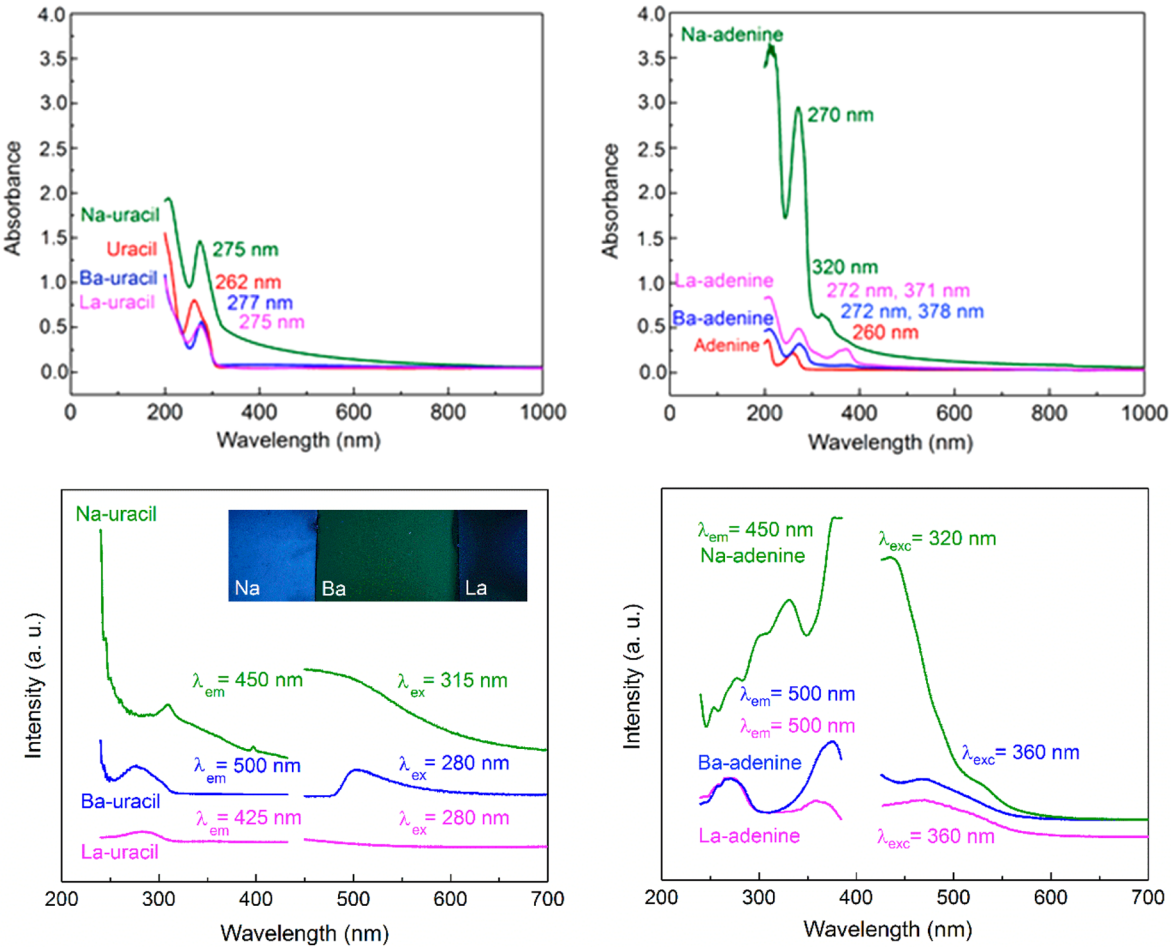

Figure 7. Upper panel: UV absorption spectra for metal-uracil (left) and metal-adenine (right) thin films and the corresponding NB precursors. Bottom panel: Fluorescence spectra for metal-uracil (left) and metal-adenine (right) thin films; the inset in the former shows the blue, green, and bluish-green fluorescence emission of Na-, Ba-, and La-uracil, respectively.

for La-adenine. Interestingly, for the two Na-based films the absorption peaks show long spectral trails extending to the visible wavelength range. This was discussed in the case of Na-uracil in our previous works and tentatively ascribed to different localized LUMO states over a certain energy range.[14,29] Apparently a somewhat similar phenomenon is here seen also for Na-adenine but not for the Ba-NB and La-NB films.

Photoluminescence excitation and emission spectra for all of the metal-NB thin-film samples are shown in the two lower panels of Figure 7. For both the uracil- and adenine series, a similar observation can be made. That is, while the spectra for Na-NB are more complex, those for Ba- and La-NB are qualitatively very similar, showing emission at the green wavelengths up to ~550 nm. However, the intensities are essentially lower for the La-NB films in comparison to those for Ba-NB. Then, for both the Na-NB films an intense fluorescence emission is seen which moreover strongly depends on the excitation wavelength. Very recently we thoroughly investigated this behavior for our Na-uracil films with time-resolved measurements and showed that the phenomenon is caused by a so-called red-edge excitation shift (REES) effect.[29] Similar experiments are planned for Na-adenine as well but not within the scope of the present work.

Finally, in order to demonstrate to suitability of our new metal-NB ALD/MLD processes for conformal coating of complex surface structures we deposited Ba-uracil films on porous anodized aluminum oxide substrate using the same deposition parameters as used in the case of flat substrates. Indeed, as can be seen from the SEM image in Figure 8 the pore walls and the bottom are completely covered with a homogeneous Ba-uracil thin film.

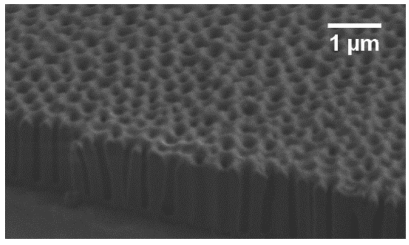

Figure 8. Cross-sectional SEM image taken at an angle of 60° XPS survey spectra for Ba-uracil coating deposited on AAO substrate.

4. CONCLUSIONS

In this work, we established a novel family of hybrid metal-nucleobase thin-film materials realized using the emerging ALD/MLD technique as a state-of-the-art synthesis tool. Our primary aim was to learn how the size and charge of the metal cation affect the growth and properties of the films. For this systematic study we selected monovalent Na, divalent Ba, and

DOI: 10.1021/acs.jpcc.7b06129
J. Phys. Chem. C 2017, 121, 17538−17545

trivalent La as the metal constituents and uracil and adenine as the NB constituents. For all six metal-NB combinations studied, smooth and homogeneous thin films were readily obtained in a highly controlled manner and with appreciably high growth rates.

The growth-per-cycle rate was found to be controlled by steric hindrance of the bulky metal-precursor ligands, the GPC value decreasing with increasing number of these ligands in the order of Na(thd), $Ba(thd)_2$, and $La(thd)_3$. Our tentative belief is that these bulky ligands may also hinder the in situ crystallization of the films, as our Na-NB films were found to be highly crystalline, Ba-NB partly crystalline, and La-NB films completely amorphous. Hence, in order to deposit crystalline ALD/MLD films for the higher-valent metal species it could be advantageous to look for precursors with as small ligands as possible.

The metal-nucleobase thin films were also characterized for their basic optical properties. In particular, both the Na-NB and Ba-NB films were found to show intense photoluminescence in blue and green wavelengths. Moreover, new phenomena were observed including the excitation-dependent emission, the details of which should be elaborated in future studies.

Our work is significant from the application point of view as well, because the ALD/MLD technique used for the synthesis permits a one-step straightforward method in producing uniform luminescent thin films with precisely controlled thicknesses. Moreover, we carried out preliminary tests on porous substrates to demonstrate that the new ALD/MLD processes yield, as expected, highly conformal coatings even on complex substrate architectures. Such luminescent nanostructures are in high demand for many advanced applications, such as sensors and organic light emitting diodes.

AUTHOR INFORMATION

Corresponding Author

*E-mail: maarit.karppinen@aalto.fi.

ORCID

Maarit Karppinen: 0000-0003-1091-1169

Notes

The authors declare no competing financial interest.

ACKNOWLEDGMENTS

The present work has received funding from the European Research Council under the European Union's Seventh Framework Programme (FP/2007-2013)/ERC Advanced Grant Agreement (No. 339478) and Academy of Finland (No. 296299). This work made use of the Aalto University Nanomicroscopy Center (Aalto-NMC) premises. Dr. Nikolay Houbenov is thanked for his guidance in AFM experiments.

REFERENCES

(1) Sanchez, C.; Boissiere, S.; Cassaignon, S.; Chaneac, C.; Durupthy, O.; Faustini, M.; Grosso, D.; Laberty-Robert, C.; Nicole, L.; Portehault, D.; Ribot, F.; Rozes, L.; Sassoye, C. Molecular Engineering of Functional Inorganic and Hybrid Materials. *Chem. Mater.* **2014**, *26*, 221−238.

(2) Steckl, A. J. DNA − a New Material for Photonics? *Nat. Photonics* **2007**, *1*, 3−5.

(3) Ko, S. H.; Su, M.; Zhang, C.; Ribbe, A. E.; Jiang, W.; Mao, C. Synergistic Self-Assembly of RNA and DNA Molecules. *Nat. Chem.* **2010**, *2*, 1050−1055.

(4) Gomez, E. F.; Venkatraman, V.; Grote, J. G.; Steckl, A. J. Exploring the Potential of Nucleic Acid Bases in Organic Light Emitting Diodes. *Adv. Mater.* **2015**, *27*, 7552−7562.

(5) Otero, R.; Xu, W.; Lukas, M.; Kelly, R. E. A.; Lægsgaard, E.; Stensgaard, I.; Kjems, J.; Kantorovich, L. N.; Besenbacher, F. Specificity of Watson−Crick Base Pairing on a Solid Surface Studied at the Atomic Scale. *Angew. Chem., Int. Ed.* **2008**, *47*, 9673−9676.

(6) Haug, A.; Schweizer, S.; Latteyer, F.; Casu, M. B.; Peisert, H.; Ochsenfeld, C.; Chasse, T. Thin Film Properties of DNA and RNA Bases; A Combined Experimental and Theoretical Study. *ChemPhysChem* **2008**, *9*, 740−747.

(7) Gardener, J. A.; Shvarova, O. Y.; Briggs, A. D.; Castell, M. R. Binary and Ternary Combination of Uracil, PTCDI, and Melamine. *J. Phys. Chem. C* **2010**, *114*, 5859−5866.

(8) Xu, W.; Tan, Q.; Yu, M.; Sun, Q.; Kong, H.; Laegsgaard, E.; Stensgaard, I.; Kjems, J.; Wang, J.-G.; Wang, C.; Besenbacher, F. Atomic-scale Structures and Interactions between the Guanine Quartet and Potassium. *Chem. Commun.* **2013**, *49*, 7210−7212.

(9) Stupp, S. I.; Palmer, L. C. Supramolecular Chemistry and Self-Assembly in Organic Materials Design. *Chem. Mater.* **2014**, *26*, 507−518.

(10) Nucleic Acid - Metal Ion Interactions. *Encyclopedia of Inorganic and Bioinorganic Chemistry*; John Wiley & Sons, Ltd.: New York, 2006.

(11) An, J.; Farha, O. K.; Hupp, J. T.; Pohl, E.; Yeh, J. I.; Rosi, N. L. Metal-Adeninate Vertices for the Construction of an Exceptionally Porous Metal-Organic Framework. *Nat. Commun.* **2012**, *3*, 604.

(12) Pratibha; Verma, S. Imine Component Based Modified Adenine Nucleobase−Metal Frameworks. *Cryst. Growth Des.* **2015**, *15*, 510−516.

(13) Soleymani, L.; Fang, Z.; Sargent, E. H.; Kelley, S. O. Programming the Detection Limits of Biosensors through Controlled Nanostructuring. *Nat. Nanotechnol.* **2009**, *4*, 844−848.

(14) Giedraityte, Z.; Lopez-Acevedo, O.; Espinosa Leal, L. A.; Pale, V.; Sainio, J.; Tripathi, T. S.; Karppinen, M. Three-Dimensional Uracil Network with Sodium as a Linker. *J. Phys. Chem. C* **2016**, *120*, 26342−26349.

(15) Nilsen, O.; Klepper, K. B.; Nielsen, H.; Fjellvåg, H. Deposition of Organic- Inorganic Hybrid Materials by Atomic Layer Deposition. *ECS Trans.* **2008**, *16*, 3−14.

(16) Dameron, A. A.; Seghete, D.; Burton, B. B.; Davidson, S. D.; Cavanagh, A. S.; Bertrand, J. A.; George, S. M. Molecular Layer Deposition of Alucone Polymer Films Using Trimethylaluminum and Ethylene Glycol. *Chem. Mater.* **2008**, *20*, 3315−3326.

(17) Peng, Q.; Gong, B.; VanGundy, R. M.; Parsons, G. N. Zincone" Zinc Oxide−Organic Hybrid Polymer Thin Films Formed by Molecular Layer Deposition. *Chem. Mater.* **2009**, *21*, 820−830.

(18) Sood, A.; Sundberg, P.; Malm, J.; Karppinen, M. Layer-by-Layer Deposition of Ti-4,4′-Oxydianiline Hybrid Thin Films. *Appl. Surf. Sci.* **2011**, *257*, 6435−6439.

(19) Sundberg, P.; Karppinen, M. Organic and Inorganic-Organic Thin Film Structures by Molecular Layer Deposition: A Review. *Beilstein J. Nanotechnol.* **2014**, *5*, 1104−1136.

(20) Nisula, M.; Karppinen, M. Atomic/Molecular Layer Deposition of Lithium Terephthalate Thin Films as High Rate Capability Li-Ion Battery Anodes. *Nano Lett.* **2016**, *16*, 1276−1281.

(21) Ahvenniemi, E.; Karppinen, M. Atomic/Molecular Layer Deposition: A Direct Gas-Phase Route to Crystalline Metal-Organic Framework Thin Films. *Chem. Commun.* **2016**, *52*, 1139−1142.

(22) Ahvenniemi, E.; Karppinen, M. In Situ Atomic/Molecular Layer-by-Layer Deposition of Inorganic−Organic Coordination Network Thin Films from Gaseous Precursors. *Chem. Mater.* **2016**, *28*, 6260−6265.

(23) Goodgame, M.; Johns, K. W. Metal Complexes of Uracil and Thymine. *J. Chem. Soc., Dalton Trans.* **1977**, 1680−1683.

(24) Karlin, K. D. *Progress in Inorganic Chemistry, Altered pKa Values of Nucleobases in Metal Complexes; Importance of Hydrogen-Bonding Interactions in Metal Nucleobases Complexes*; John Wiley Sons, Inc.: Hoboken, NJ, 2005; Vol. *54*.

DOI: 10.1021/acs.jpcc.7b06129
J. Phys. Chem. C 2017, 121, 17538−17545

(25) Nowak, M. J.; Lapinski, L.; Kwiatkowski, J. S.; Leszczynski, J. Molecular Structure and Infrared Spectra of Adenine. Experimental Matrix Isolation and Density Functional Theory Study of Adenine 15N Isotopomers. *J. Phys. Chem.* **1996**, *100*, 3527−3534.
(26) Haug, A.; Schweizer, S.; Latteyer, F.; Casu, M. B.; Peisert, H.; Ochsenfeld, C.; Chassé, T. Thin-Film Properties of DNA and RNA Bases: A Combined Experimental and Theoretical Study. *ChemPhysChem* **2008**, *9*, 740−747.
(27) Papageorgiou, A. C.; Fischer, S.; Reichert, J.; Diller, K.; Blobner, F.; Klappenberger, F.; Allegretti, F.; Seitsonen, A. P.; Barth, J. V. Chemical Transformations Drive Complex Self-Assembly of Uracil on Close-Packed Coinage Metal Surfaces. *ACS Nano* **2012**, *6*, 2477−2486.
(28) Peeling, J.; Hruska, F. E.; McKinnon, D. M.; Chauhan, M. S.; McIntyre, N. S. ESCA Studies of the Uracil Base. The Effect of Methylation, Thionation, and Ionization on Charge Distribution. *Can. J. Chem.* **1978**, *56*, 2405−2411.
(29) Pale, V.; Giedraityte, Z.; Chen, X.; Lopez-Acevedo, O.; Tittonen, I.; Karppinen, M. Excitation-dependent Fluorescence from Atomic/Molecular Layer Deposited Sodium-Uracil Thin Films. *Sci. Rep.* **2017**, *7*, 6982.

DOI: 10.1021/acs.jpcc.7b06129
J. Phys. Chem. C 2017, 121, 17538−17545